

Figure 6 Comparison between measured and simulated results

ACKNOWLEDGMENT

The authors acknowledge the Directorate of Research and Development (DRD), Defence Science and Technology Agency (DSTA), Republic of Singapore, for funding of this project.

REFERENCES

1. L. Lecheminoux and N. Gosselin, Advanced design, technology and manufacturing for high volume and low cost production, In: Electronics Manufacturing Technology Symposium, July, 2003, pp. 255–260.
2. O.K. Lim, Y.J. Kim, and S.S. Lee, A compact integrated combline band pass filter using LTCC technology for C-band wireless applications, In: 33rd European Microwave Conference, Vol. 1, (2003) pp. 203–206.
3. L.K. Yeung and K.L. Wu, A compact second-order LTCC bandpass filter with two finite transmission zeros, IEEE Trans Microwave Theory Tech 51 (2003), 337–341.
4. A. Sutono, D. Heo, Y.J. Emery Chen, and J. Laskar, High-Q LTCC-based passive library for wireless system-on-package (SOP) module development, IEEE Trans Microwave Theory Tech 49 (2001), 1715–1724.
5. R.M. Joao, F. Le-Strat, P.F. Alleaume, V.J. Caldinhas, J. Schroth, T. Muller, and F.J. Costa, Low cost LTCC filters for a 30GHz satellite system, In: 33rd European Microwave Conference (2003), pp. 817–820.
6. B.T. Tan, J.J. Yu, S.T. Chew, M.S. Leong, and B.L. Ooi, A miniaturized dual-mode ring bandpass filter with a new perturbation, IEEE Trans Microwave Theory Tech 53 (2005), 343–348.
7. M. Matsuo, H. Yabuki, and M. Makimoto, Dual-mode stepped-impedance ring resonator for bandpass filter applications, IEEE Trans Microwave Theory Tech 49 (2001), 1235–1240.
8. K. Chang, Microwave ring circuits and antennas, Wiley, New York, 1996, Ch. 6.
9. B.T. Tan, J.J. Yu, S.T. Chew, M.S. Leong, and B.L. Ooi, A dual-mode bandpass filter on perforated ground, In: Proceedings of Asia-Pacific Microwave Conference (2003), pp. 797–800.
10. B.T. Tan, S.T. Chew, M.S. Leong, and B.L. Ooi, A modified microstrip circular patch resonator filter, IEEE Microwave Wireless Compon Lett 12 (2002), 252–254.

© 2006 Wiley Periodicals, Inc.

INTERNAL PIFAS FOR UMTS/WLAN/WiMAX MULTI-NETWORK OPERATION FOR A USB DONGLE

Wei-Cheng Su and Kin-Lu Wong

Department of Electrical Engineering,
National Sun Yat-Sen University,
Kaohsiung 804, Taiwan

Received 30 March 2006

ABSTRACT: Two kinds of internal planar inverted-F antennas (PIFAs) suitable for application in a USB dongle for UMTS/WLAN/WiMAX multi-network operation are presented. The first one is a hybrid PIFA consisting of a metal-plate portion and a printed portion, while the second one is a printed PIFA. Both the hybrid and printed PIFAs are suitable to be mounted at the top no-ground region of the USB dongle as internal antennas and can generate two wide bandwidths at about 2.3 and 5.5 GHz to cover the UMTS (1920–2170 MHz), WLAN (2400–2484/5150–5350/5725–5825 MHz) and WiMAX (2500–2690/5150–5850 MHz) bands for seamless wireless network access. Detailed designs of the two PIFAs are described, and results of their impedance and radiation characteristics are presented and discussed. © 2006 Wiley Periodicals, Inc. Microwave Opt Technol Lett 48: 2249–2253, 2006; Published online in Wiley InterScience (www.interscience.wiley.com). DOI 10.1002/mop.21903

Key words: antennas; PIFAs; USB dongles; UMTS antennas; WLAN antennas; WiMAX antennas

1. INTRODUCTION

Conventional USB (Universal Serial Bus) dongles [1] are attractive for providing the plug-and-play function in mobile communication devices such as the laptops. With internal antennas embedded in the USB dongle, convenient wireless network access for mobile devices can also be provided. This kind of wireless USB dongle is becoming very attractive for wireless users. For this perspective trend, promising internal antennas for the USB dongle are greatly demanded. However, although a variety of internal antennas have been reported for application in mobile devices [2], the promising internal antennas for the USB dongle applications are relatively very few in the published literature.

In this paper, we present two promising internal PIFAs suitable for application in the USB dongle for UMTS (Universal Mobile Telecommunication System, 1920–2170 MHz), WLAN (Wireless Local Area Network, 2400–2484/5150–5350/5725–5825 MHz), and WiMAX [3] (Worldwide Interoperability for Microwave Access, 2500–2690/5150–5850 MHz) multi-network operation to provide seamless network access for wireless users. Both the two promising PIFAs (one denoted as the hybrid PIFA with metal-plate and printed portions and the other as the printed PIFA) are with compact dimensions and suitable to be mounted at the top no-ground region of the USB dongle as internal antennas. Details of the design considerations of the proposed hybrid and printed PIFAs are described. Experimental results of the constructed prototypes are also presented and discussed.

2. DESIGN CONSIDERATIONS OF TWO PROPOSED PIFAS

2.1 The Hybrid PIFA

Figure 1(a) shows the geometry of the proposed hybrid PIFA mounted at the top no-ground region (size $5 \times 20 \text{ mm}^2$) of the USB dongle. In the figure, the system ground plane of the USB dongle is selected to be of width 20 mm and length 50 mm, which are reasonable dimensions of general USB dongles. Note that the

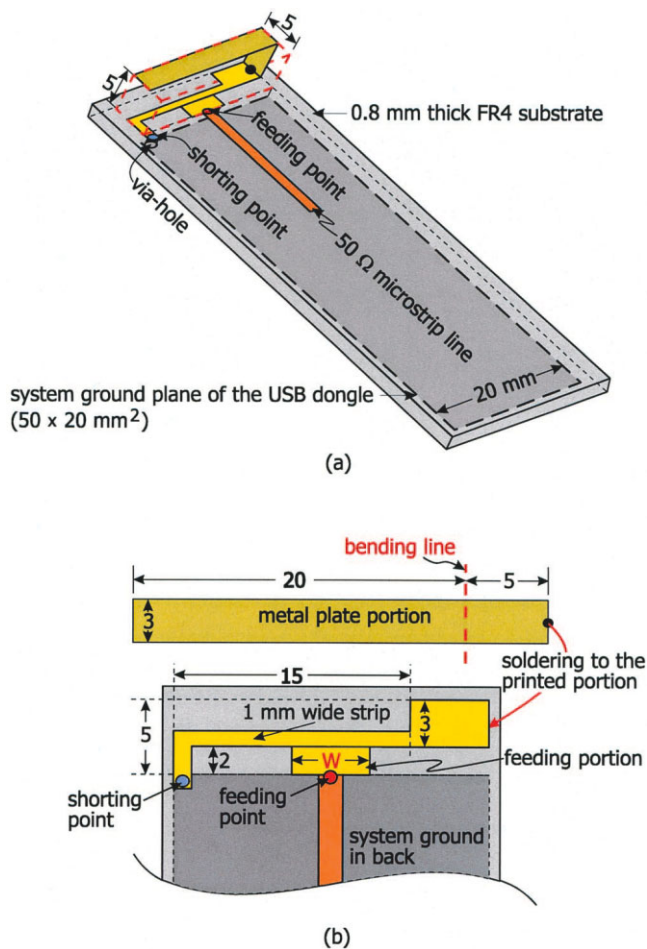


Figure 1 (a) Configuration of the proposed hybrid PIFA applied in a USB dongle. (b) Detailed dimensions of the metal-plate portion and printed portion in the hybrid PIFA. [Color figure can be viewed in the online issue, which is available at www.interscience.wiley.com]

system ground plane is printed on the back side of a 0.8 mm thick FR4 substrate in this study, which can be considered as the system circuit board of the practical USB dongle. The hybrid PIFA consists of a printed portion and a metal-plate portion. The printed portion is printed on the top no-ground region of the FR4 substrate and occupies a small area of 5 × 20 mm². Note that the printed portion is of an inverted-F shape [4–6] with its end portion widened for connecting to the bent metal-plate portion arranged to be on top of the printed portion with a height of 5 mm. For the metal-plate portion, it is easily fabricated from bending a simple rectangular strip of width 3 mm and length 25 mm [see Figure 1(b)]. In the study, a 0.2 mm thick copper plate is used for fabricating the metal-plate portion. The printed and metal-plate portions together occupy a compact volume of 5 × 5 × 20 mm³, which allows it to be easily concealed within the casing of the general USB dongle as an internal antenna.

Also note that the printed portion is short-circuited to the system ground plane through a via-hole in the 0.8 mm thick FR4 substrate and has a central feeding portion of width W and length 2 mm. A 50 Ω microstrip feedline printed on the front surface of the FR4 substrate is connected to the central feeding portion of the hybrid PIFA at the feeding point to test the antenna in the experiment. With the presence of the metal-plate portion, the effective resonant path of the proposed hybrid PIFA is greatly lengthened. In this design, the required length from the feeding point to the

open end of the metal-plate portion can be roughly determined from one-quarter wavelength of the desired center frequency (about 2.3 GHz) of the lower operating band in this study. Also, in order to achieve a better impedance matching, the printed portion is adjusted to be with a non-uniform strip in width (from 1 to 3 mm in width). Further note that the upper operating band of the hybrid PIFA is the antenna's second resonant mode, which is found to be effectively controlled by the width W of the central feeding portion (the optimal width for W is 7 mm for the hybrid PIFA in this study). The desired antenna's second (upper) operating band in this study is at about 5.5 GHz, and detailed effects of the width W on controlling this operating band are analyzed with the aid of Figure 5 in Section 3. With the proposed hybrid PIFA, two wide operating bands at about 2.3 and 5.5 GHz can be excited to cover the UMTS/WLAN/WiMAX multi-network operation.

2.2 The Printed PIFA

Figure 2(a) shows the geometry of the proposed printed PIFA for application in a USB dongle. With comparison to the hybrid PIFA described in Section 2.1, the printed PIFA can be treated as replacing the metal-plate portion in the hybrid PIFA by a second printed portion of size 7 × 20 mm² on the FR4 substrate. In this case, the whole structure of the proposed printed PIFA here can be implemented by printing on the FR4 substrate, yet two wide operating bands at about 2.3 and 5.5 GHz for UMTS/WLAN/

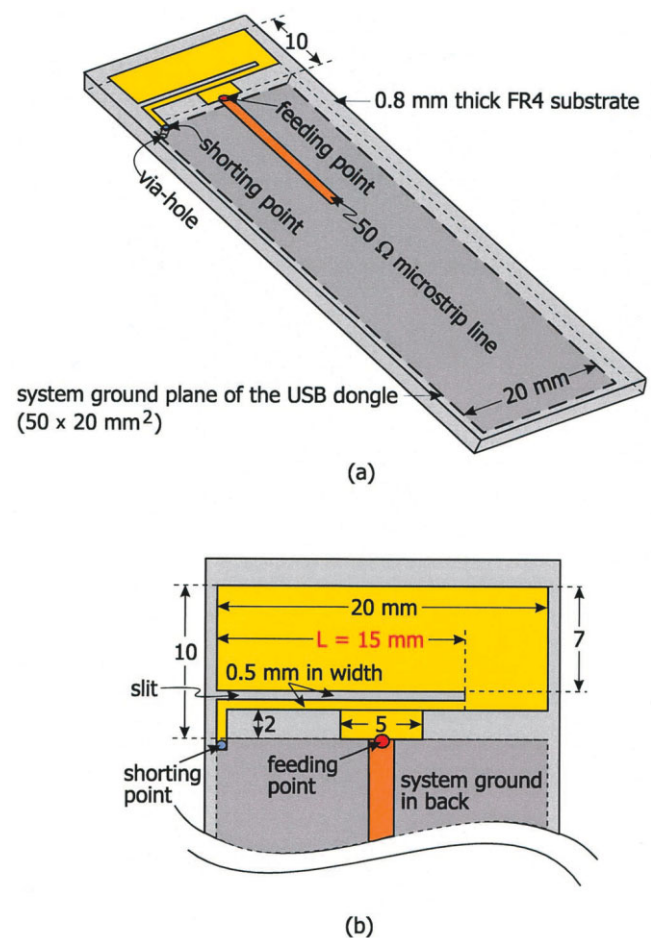


Figure 2 (a) Configuration of the proposed printed PIFA applied in a USB dongle. (b) Detailed dimensions of the printed PIFA. [Color figure can be viewed in the online issue, which is available at www.interscience.wiley.com]

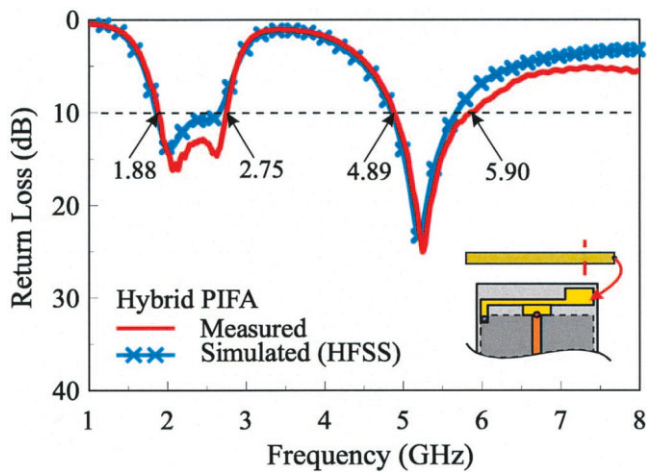


Figure 3 Measured and simulated return loss of the hybrid PIFA with $W = 7$ mm. [Color figure can be viewed in the online issue, which is available at www.interscience.wiley.com]

WiMAX multi-network operation can still be obtained. Details of the dimensions of the proposed printed PIFA are given in Figure 2(b). Note that the total protruded length of the printed PIFA reaches 10 mm, which is two times that of the hybrid PIFA studied in Figure 1. Please also note that there is a narrow slit of width 0.5 mm and length L in the printed PIFA, which can effectively meander the antenna's excited surface current path and lower the antenna's fundamental resonant frequency. Hence, by selecting a proper length L (15 mm here), the lower operating band of the printed PIFA can be excited at about the desired frequency 2.3 GHz. By further incorporating a proper width W of the feeding portion (5 mm here), good impedance matching for frequencies over the two (lower and upper) wide operating bands of the printed PIFA at about 2.3 and 5.5 GHz can be obtained. Detailed effects of the slit length L on the performances of the printed PIFA will be discussed in Section 3 with the aid of Figure 6.

3. RESULTS AND DISCUSSION

The proposed hybrid PIFA shown in Figure 1 with $W = 7$ mm was first constructed and tested. Figure 3 shows the measured and

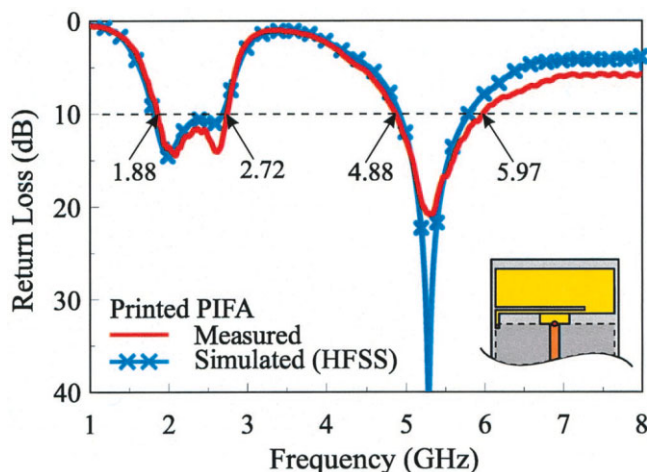


Figure 4 Measured and simulated return loss of the printed PIFA with $L = 15$ mm. [Color figure can be viewed in the online issue, which is available at www.interscience.wiley.com]

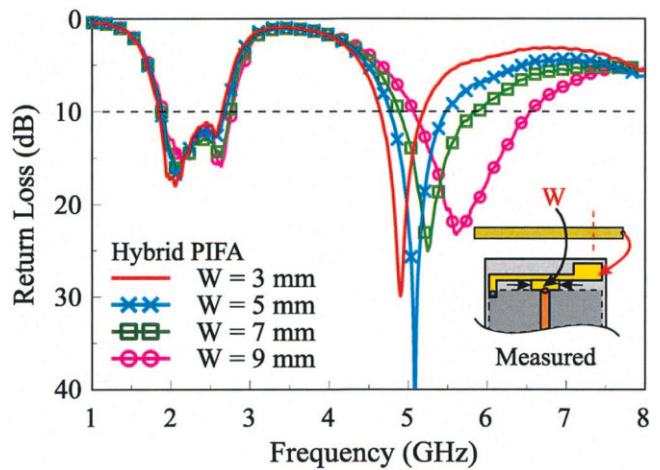


Figure 5 Measured return loss as a function of the feeding-portion width w ; other parameters are the same as given in Figure 1. [Color figure can be viewed in the online issue, which is available at www.interscience.wiley.com]

simulated return loss. The simulated results are obtained from Ansoft simulation software HFSS (High Frequency Structure Simulator) [7], and agreement between the simulation and measurement is seen. As expected, two wide operating bands at about 2.3 and 5.5 GHz are obtained. The measured impedance bandwidths of the lower and upper operating bands, defined by 10 dB return loss, reach 870 MHz (1880–2750 MHz) and 1010 MHz (4890–5900 MHz), respectively, which cover the desired UMTS/WLAN/WiMAX multi-network operation.

The proposed printed PIFA shown in Figure 2 with $L = 15$ mm was also constructed and tested. Figure 4 shows the measured and simulated return loss, and two wide operating bands at about 2.3 and 5.5 GHz are also excited. Good agreement between the measurement and simulation is also achieved. The obtained impedance bandwidths are similar to those shown in Figure 3 for the hybrid PIFA. That is, similar impedance matching characteristics for the printed and hybrid PIFAs are obtained. In this case, the measured impedance bandwidths reach 840 MHz (1880–2720 MHz) and 1090 MHz (4880–5970 MHz) for the lower and upper operating bands, respectively.

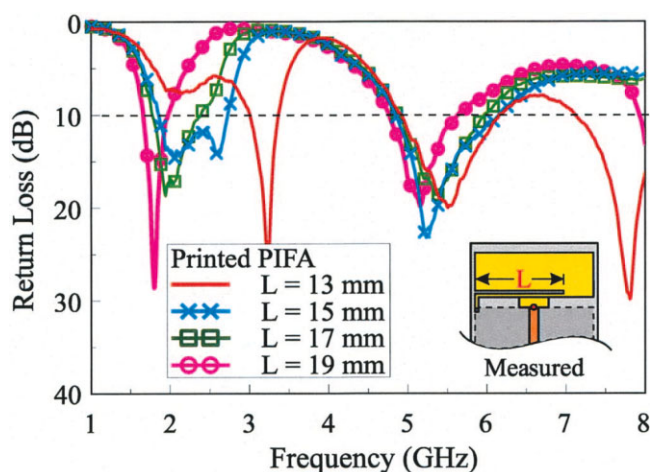


Figure 6 Measured return loss as a function of the slit length L ; other parameters are the same as given in Figure 2. [Color figure can be viewed in the online issue, which is available at www.interscience.wiley.com]

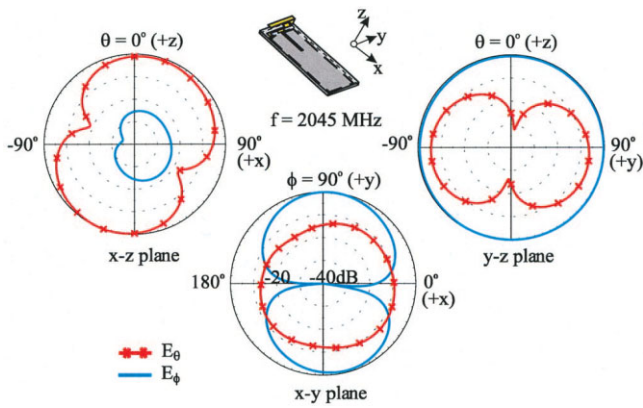


Figure 7 Measured radiation patterns at 2045 MHz for the hybrid PIFA studied in Figure 3. [Color figure can be viewed in the online issue, which is available at www.interscience.wiley.com]

Effects of the feeding-portion width W on the impedance matching of the hybrid PIFA are studied in Figure 5. Results indicate that very small variations for the lower operating band are obtained. On the other hand, for the upper operating band, significant effects of the width W are seen. This suggests that, by varying the width W , the upper band of the proposed hybrid PIFA can be easily adjusted without affecting the lower band. As for adjusting the lower band, one can vary the length of the metal-plate portion mounted above the antenna's printed portion, which varies the resonant length of the fundamental resonant mode of the hybrid PIFA. This characteristic has been described in Section 2.1. Hence, by varying the width W and the length of the metal-plate portion, easy adjustment of the antenna's two operating bands can be achieved. Also note that, in this study, the width W is chosen to be 7 mm to cover the required bandwidths of the WLAN and WiMAX operations in the 5 GHz band.

Figure 6 studies the effects of slit length L on the impedance matching of the printed PIFA. Measured results of the return loss for the cases with various slit lengths of $L = 13$ to 19 mm are presented. It is seen that, by increasing the slit length L , the antenna's lower band can be excited at lower frequencies. For the upper band, however, smaller effects of the slit length L are seen. From the results obtained, the slit length L for the printed PIFA is selected to be 15 mm. In this case, the maximum bandwidth for the lower band is obtained.

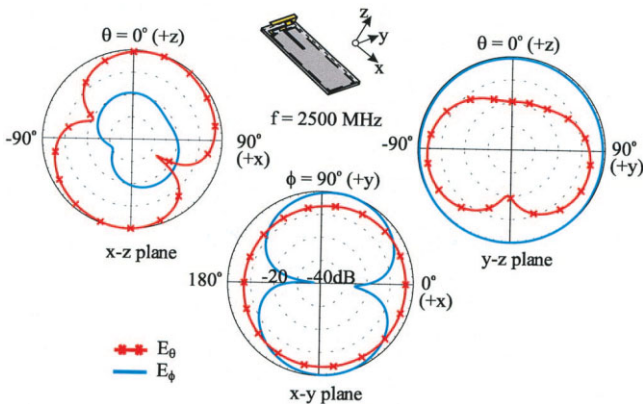


Figure 8 Measured radiation patterns at 2500 MHz for the hybrid PIFA studied in Figure 3. [Color figure can be viewed in the online issue, which is available at www.interscience.wiley.com]

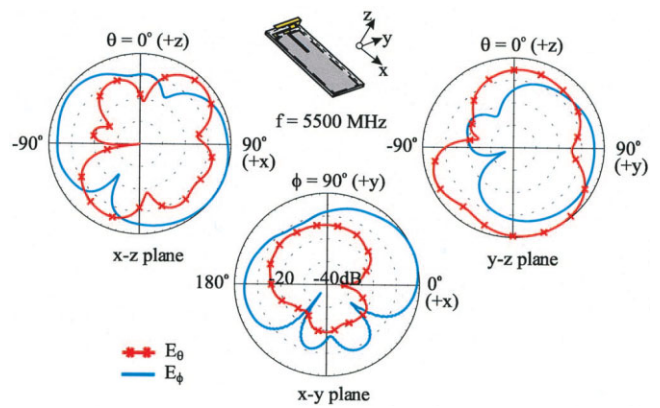


Figure 9 Measured radiation patterns at 5500 MHz for the hybrid PIFA studied in Figure 3. [Color figure can be viewed in the online issue, which is available at www.interscience.wiley.com]

The radiation characteristics of the constructed hybrid and printed PIFAs were also studied. Figures 7, 8, and 9 show the measured radiation patterns at 2045, 2500, and 5500 MHz for the hybrid PIFA studied in Figure 3. In general, the radiation patterns

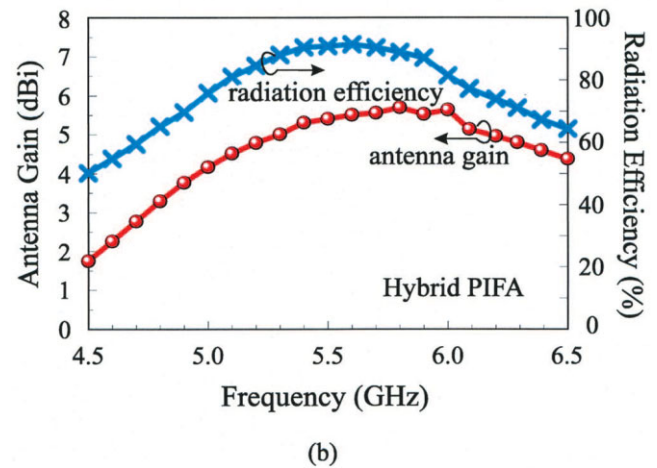
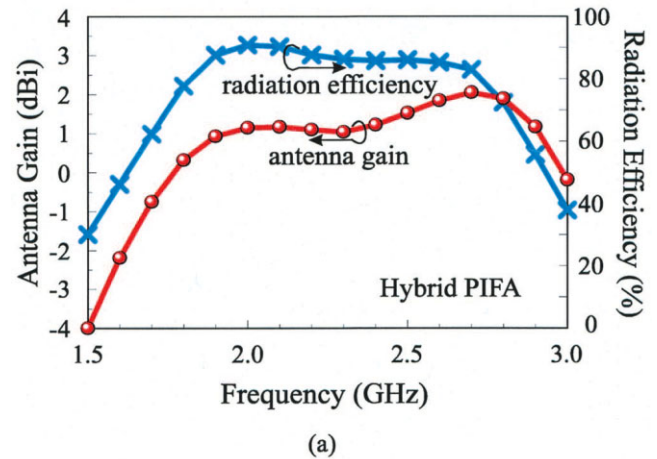
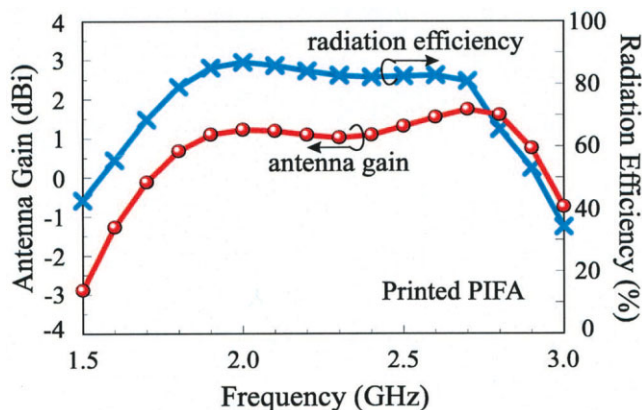
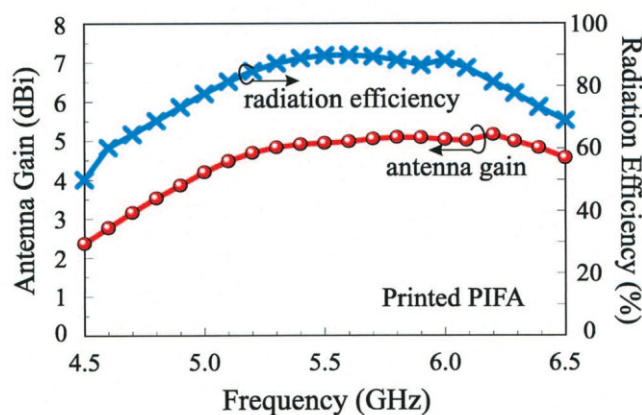


Figure 10 Measured antenna gain and simulated radiation efficiency for the hybrid PIFA studied in Figure 3. (a) The lower band. (b) The upper band. [Color figure can be viewed in the online issue, which is available at www.interscience.wiley.com]



(a)



(b)

Figure 11 Measured antenna gain and simulated radiation efficiency for the hybrid PIFA studied in Figure 4. (a) The lower band. (b) The upper band. [Color figure can be viewed in the online issue, which is available at www.interscience.wiley.com]

of the printed PIFA show no special distinction when compared with those of the hybrid PIFA shown here. Thus, the radiation patterns of the printed PIFA are not shown for brevity.

Figure 10 presents the measured antenna gain and simulated radiation efficiency over the lower and upper bands of the hybrid PIFA studied in Figure 3. For the lower band from 1.88 to 2.75 GHz, the antenna gain is varied in the range of 1.3–2.5 dBi, while the radiation efficiency is about 85% over the band. As for the upper band from 4.89 to 5.90 GHz, the antenna gain is varied from about 4.1 to 5.5 dBi, and the radiation efficiency is also about 85% over the band. The corresponding results of the printed PIFA studied in Figure 4 are shown in Figure 11. It can be seen that the obtained antenna gain and radiation efficiency are about the same as those shown in Figure 10. That is, similar radiation characteristics of the hybrid and printed PIFAs studied here are obtained.

4. CONCLUSION

Two kinds of promising PIFAs (hybrid PIFA and printed PIFA) for application in a USB dongle have been proposed, fabricated, and tested. Both the hybrid and printed PIFAs occupy a compact volume and can easily be embedded inside the casing of the general USB dongle as internal antennas. In addition, both the two PIFAs can provide two wide operating bands for covering UMTS/

WLAN/WiMAX multi-network operation. Easy adjustment of the two wide operating bands of the proposed hybrid and printed PIFAs has also been obtained. The two PIFAs also show good radiation characteristics over their two wide operating bands.

ACKNOWLEDGMENT

This work is partially supported by the Aim for Top University Plan of the Ministry of Education, Taiwan, Republic of China.

REFERENCES

1. Wikipedia, <http://en.wikipedia.org/wiki/USB>.
2. K.L. Wong, Planar antennas for wireless communications, Wiley, New York, 2003.
3. Worldwide Interoperability for Microwave Access Forum or WiMAX Forum, <http://www.wimaxforum.org>.
4. C.M. Su, K.L. Wong, W.S. Chen, and Y.T. Cheng, A microstrip-coupled printed inverted-F monopole antenna, *Microwave Opt Technol Lett* 43 (2004), 470–472.
5. M. Ali and G.J. Hayes, Small printed integrated inverted-F antenna for Bluetooth application, *Microwave Opt Technol Lett* 33 (2002), 347–349.
6. Y.L. Kuo, T.W. Chiou, and K.L. Wong, A novel dual-band printed inverted-F antenna, *Microwave Opt Technol Lett* 31 (2001), 353–355.
7. <http://www.ansoft.com/products/hf/hfss/>, Ansoft Corporation HFSS.

© 2006 Wiley Periodicals, Inc.

A NOVEL MICROSTRIP LOWPASS FILTER HAVING TWO TRANSMISSION ZEROS TO GET SHARP ATTENUATION AND WIDE STOPBAND

Jingyan Mo,¹ Wei Liu,¹ and Zhewang Ma²

¹ School of Communication and Information Engineering
Shanghai University
China

² Department of Electrical and Electronic Systems
Saitama University
Japan

Received 30 March 2006

ABSTRACT: This paper proposes a novel microstrip four-pole lowpass filter with compact size and excellent frequency property. Two transmission zeros are introduced in its stopband. The first transmission zero is produced nearby the passband and makes a sharp rate of attenuation. The second transmission zero is introduced to increase significantly the stopband width. The positions of the two transmission zeros can be adjusted easily. Although it has a smaller number of circuit elements and a lower insertion loss, the filter shows a frequency response better than that of a five-pole elliptic function filter. The measured filtering characteristics of the filter agree excellently with the simulated results. © 2006 Wiley Periodicals, Inc. *Microwave Opt Technol Lett* 48: 2253–2256, 2006; Published online in Wiley InterScience (www.interscience.wiley.com). DOI 10.1002/mop.21902

Key words: microstrip line; low-pass filter; cross-coupling; transmission zero

1. INTRODUCTION

Microstrip lowpass filters (LPFs) are used in many microwave circuits, such as oscillators and duplexers. Conventional L–C ladder type LPFs are usually realized by cascading short lengths of high and low impedance microstrip lines alternately. The microstrip stepped-impedance LPF is simple in structure and easy to